Identification of Early Carboniferous Granitoids from Southern Tibet and Implications for Terrane Assembly Related to the Paleo-Tethyan Evolution

Wei-Qiang Ji,[1,*] *Fu-Yuan Wu,*[1] *Sun-Lin Chung,*[2] *and Chuan-Zhou Liu*[1]

1. State Key Laboratory of Lithospheric Evolution, Institute of Geology and Geophysics, Chinese Academy of Sciences, P.O. Box 9825, Beijing 100029, China; 2. Department of Geosciences, National Taiwan University, Taipei 10617, Taiwan

ABSTRACT

This article presents zircon U-Pb and Hf isotope data, together with the whole-rock major- and trace-element composition, of Early Carboniferous granitoids newly identified from the Jiacha and Langxian areas in the southern Lhasa terrane, southern Tibet. The Jiacha rocks are monzogranites that yield zircon U-Pb ages of 347–345 Ma and $\varepsilon_{Hf}(t)$ values from −5.4 to −4.9. The Langxian rocks are granodiorites with slightly older zircon U-Pb ages of 355–352 Ma and lower $\varepsilon_{Hf}(t)$ values from −6.8 to −6.5. Our data suggest that these granitoids were generated largely by reworking of Paleoproterozoic (T_{DM}^{C} = 1.78–1.67 Ga) basement materials. In conjunction with literature data, it is further argued that the southern and central parts of the Lhasa terrane, separated by the Sumdo eclogite belt, should have been an integrated block before the late Paleozoic. Our study supports the notion that the Lhasa terrane was derived from the northern margin of Gondwanaland, in association with formation of at least two stages of Tethyan Ocean basins, now exposed as the Sumdo belt and the Indus-Tsangpo suture.

Online enhancements: appendix tables.

Introduction

As a major component of southern Tibet, the Lhasa terrane is characterized by widespread Mesozoic-Cenozoic magmatic rocks that have attracted extensive study (Schärer et al. 1984; Coulon et al. 1986; Chung et al. 2003; Mo et al. 2005; Chu et al. 2006; Wen et al. 2008; Ji et al. 2009*a*, 2009*b*; Lee et al. 2009; Zhu et al. 2011*b*; and references therein). However, research on late Paleozoic magmatic activity has been focused in the central Lhasa terrane (Geng et al. 2007, 2009; Zhu et al. 2009*b*, 2010), because of the scarcity of Paleozoic magmatic records elsewhere. Existing data suggest that Carboniferous volcanosedimentary sequences were formed in a marginal-rifting setting (Geng et al. 2007), while Permian volcanic rocks have been interpreted as arc-like products generated in a subduction setting (Geng et al. 2009; Zhu et al. 2010). In conjunction with the discovery of the Sumdo eclogite (metamorphism age of ca. 262 Ma), which shows mid-ocean ridge basalt (MORB) geochemical affinities (Yang et al. 2009), Zhu et al. (2010) further argued that closure of this "Sumdo" oceanic basin and subsequent terrane amalgamation resulted in the Pikang granite (ca. 263 Ma) in the central Lhasa terrane. However, the evolution of this branch of the paleo-Tethys remains enigmatic; fundamental problems, such as how long the ocean floor spreading lasted and when subduction began, still persist. These issues await further detailed studies on the late Paleozoic geological records in the Lhasa terrane.

In this article, we present zircon U-Pb ages and Hf isotopes, together with whole-rock major- and trace-element data, of Early Carboniferous granitoids newly identified from the southern Lhasa terrane. Combining these with literature data, we propose new interpretations not only of the magmatic and tectonic evolution of the Lhasa terrane but also

Manuscript received June 3, 2011; accepted March 30, 2012.
* Author for correspondence; e-mail: jiweiqiang@mail.iggcas.ac.cn.

[The Journal of Geology, 2012, volume 120, p. 531–541] 0022-1376/2012/12005-0003$15.00. DOI: 10.1086/666742

of its implications for the Gondwana dispersion and paleo-Tethys reconstruction.

Geological Background and Samples

The Tibetan Plateau consists of four major terranes: from south to north, the Himalayas (the northernmost part of India), Lhasa, Qiangtang, and Songpan-Ganze (fig. 1*A*), separated by the Indus-Tsangbo, Bangong-Nujiang, and Jinsha sutures, respectively (Şengör et al. 1988; Yin and Harrison 2000). The Lhasa terrane is an east-west-trending tectonic-magmatic belt, with a width ranging from less than 100 km to 300 km, that can be subdivided into two (Yang et al. 2009) or three (Zhu et al. 2010) parts in the north-south direction. The southern Lhasa terrane is intruded by the Mesozoic-Cenozoic Gangdese batholith (Chu et al. 2006; Wen et al. 2008; Ji et al. 2009*a*; Zhu et al. 2011*b*) and covered by coeval volcanic rocks and associated sedimentary formations (Coulon et al. 1986; He et al. 2007; Lee et al. 2007, 2009; Zhu et al. 2008, 2009*b*), while the northern part consists mainly of Jurassic-Cretaceous sedimentary and igneous rocks (Zhu et al. 2010 and references therein). The central Lhasa terrane comprises Ordovician-Cenozoic volcanosedimentary sequences (Pan et al. 2004; Kang et al. 2008; Zhu et al. 2009*a*, 2010, 2011*a*) and Permian-Eocene granitic rocks (Chu et al. 2006; Wen et al. 2008; Zhu et al. 2009*c*, 2010, 2011*b* and references therein). Precambrian basement is rarely identified, now exposed only west of Nam Tso in the central Lhasa terrane (Hu et al. 2005; Zhang et al. 2010; Dong et al. 2011), as the Amdo microcontinent

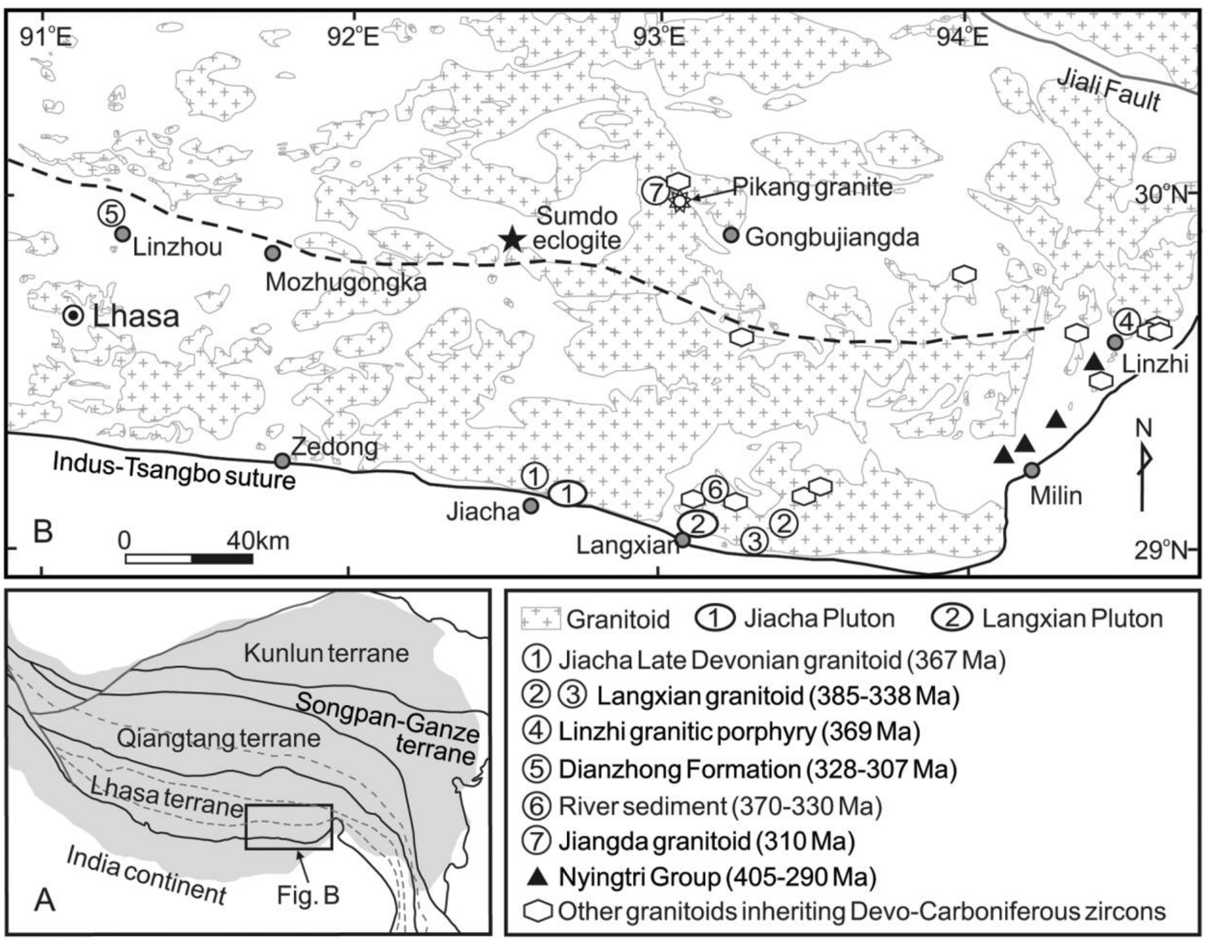

Figure 1. *A*, Location of the study region in the Tibetan Plateau. *B*, Outcrops of granitoids in the eastern Lhasa terrane. The dashed line marks the boundary between the southern and central Lhasa terranes, along which the Sumdo eclogite (star) is exposed. Other symbols are given in the key, with the inherited or detrital zircon ages in parentheses. Data sources include Quidelleur et al. (1997), Chu et al. (2006), Lee et al. (2007), Wen et al. (2008), Chung et al. (2009), Zhang et al. (2009), Zhu et al. (2009*b*, 2011*b*), Dong et al. (2010*a*), and Ji (2010). A color version of this figure is available in the online edition or from the *Journal of Geology* office.

should separated from the Lhasa terrane on the basis of the new study (Zhu et al. 2011*c*).

This study reports granitic rocks collected near Jiacha and Langxian counties from the southern margin of the Gangdese batholith (fig. 1*B*). The Jiacha pluton is composed of monzogranites (samples JC01-1, 09FW54, and 09FW55) with medium- to coarse-grained texture (fig. 2*A*). The Langxian pluton consists mainly of medium-grained granodiorites (samples 09FW36, 09FW39, and ML12-1), together with a minor dioritic enclave (sample 09FW35) and a felsic dike (sample 09FW37). The Jiacha and Langxian granitoids both develop gneissic structure and local mylonitic structure (fig. 2*B*). Their mineral assemblages are similar, with quartz, K-feldspar, plagioclase, biotite, and minor accessory minerals, such as zircon. The dioritic enclave has more abundant biotite and is finer in grain size. The felsic dike has a mineral assemblage of quartz, K-feldspar, muscovite, and subordinate biotite.

Analytical Methods

Zircon crystals were separated by heavy-liquid and magnetic separation techniques from crushed rocks, and individual crystals were hand-picked. Zircons were mounted in epoxy resin and polished to remove the upper third of each grain. All analyses were performed at the Institute of Geology and Geophysics, Chinese Academy of Sciences. Cathodoluminescence images were used for grain selection. For zircon grains larger than 50–60 μm, U-Pb dating and Hf isotopic analysis were carried out simultaneously by laser ablation–inductively coupled plasma mass spectrometry (LA-ICPMS), using an Agilent 7500a quadruple ICPMS and a Thermo-Finnigan Neptune multicollector (MC) ICPMS connected to a 193-nm excimer ArF laser ablation system (Geolas Plus). The detailed analytical procedures can be found in Xie et al. (2008). Replicated zircon U-Pb dating was performed for some samples via secondary-ion mass spectrometry (SIMS), following the analytical procedures described by Li et al. (2009*a*). For zircon grains smaller than 50 μm, in situ Hf isotopic analyses were performed on the dated spots by the MC ICPMS method (Wu et al. 2006). The zircon U-Pb LA-ICPMS, SIMS, and Hf isotopic data are listed in tables A1–A3, respectively, available in the online edition or from the *Journal of Geology* office. The results are sum-

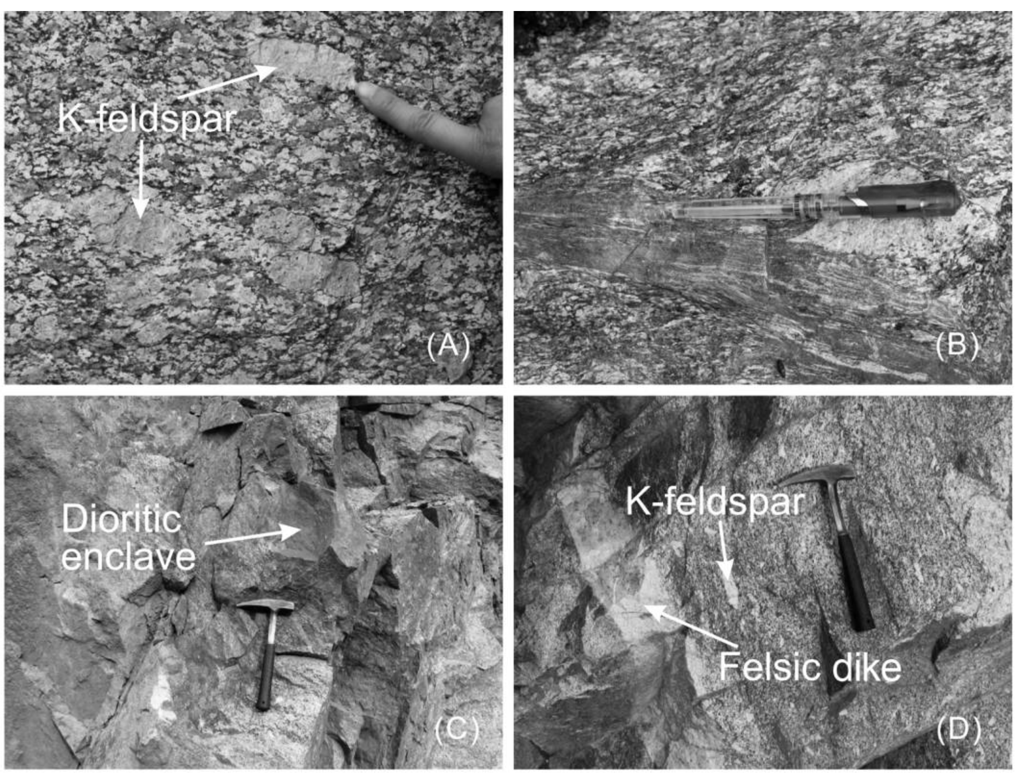

Figure 2. Field photographs of Jiacha and Langxian plutons. *A*, Jiacha monzogranite; *B*, local mylonite structure of Jiacha pluton; *C*, dioritic enclave from Langxian pluton; *D*, Langxian pluton and its felsic dike. A color version of this figure is available in the online edition or from the *Journal of Geology* office.

marized in table 1, and U-Pb concordia diagrams are presented in figure 3. Major elements were measured by x-ray fluorescence spectrometry (PANalytical Axios) at the Institute of Geology and Geophysics, with an analytical uncertainty of <0.5%. Trace elements were determined by the ICPMS (Agilent 7500a) method at the China University of Geosciences (Wuhan), following Liu et al. (2008). The routine analytical precision and accuracy for most trace elements measured are estimated to be <5%. Major- and trace-element results are summarized in table A4, available in the online edition or from the *Journal of Geology* office, and presented in figure 4.

Analytical Results

Zircon U-Pb Ages. Most zircon separates from the Jiacha and Langxian plutons are euhedral and show long to short prismatic shapes, with lengths of 80–200 μm, length/width ratios of 1.5–3, and well-developed oscillatory zoning. For the Jiacha pluton, U-Pb ages obtained by the LA-ICPMS (JC01-1: 345.3 ± 2.6 Ma; range 336–354 Ma) and SIMS (09FW55: 346.7 ± 2.7 Ma) methods are identical. The Langxian granodiorites yield slightly older ages of 355.1 ± 4.2 Ma (09FW36) and 352.0 ± 3.1 Ma (ML12-1) by LA-ICPMS and 353.5 ± 2.6 Ma (ML12-1) by SIMS. The spot ages of zircons from the Langxian pluton give a range of 344–363 Ma. Zircons from the felsic dike are smaller in grain size (40–100 μm) than those of the host granodiorites of the Langxian pluton, while those from the dioritic enclave have higher length/width ratios of 3–5 and lengths of 100–300 μm. The dioritic enclave (09FW35) yields $^{206}Pb/^{238}U$ ages of 353.5 ± 3.2 Ma, with a range of 339–367 Ma (LA-ICPMS) and 355.5 ± 2.8 Ma (SIMS), while the felsic dike (09FW37) gives similar ages of 352.1 ± 6.9 Ma (range 346–359 Ma; LA-ICPMS) and 354.1 ± 2.9 Ma (SIMS). Therefore, the dioritic enclave and the felsic dike from Langxian pluton show ages identical to that of the host granodiorite (table 1; fig. 3).

Zircon Hf Isotopes. The zircon $\varepsilon_{Hf}(t)$ values of samples JC01-1 and 09FW55 from the Jiacha pluton are −5.4 ± 0.4 (range −7.0 to −3.6) and −4.9 ± 0.5 (range −6.8 to −2.6), respectively, whereas the Langxian granodiorites exhibit slightly lower $\varepsilon_{Hf}(t)$ values from −6.5 ± 0.7 (ML12-1: range −9.0 to −3.2) to −6.8 ± 0.4 (09FW36: range −8.1 to −4.5; table 1). Similar zircon $\varepsilon_{Hf}(t)$ values are observed in the dioritic enclave and felsic dike, −5.8 ± 0.7 (09FW35: range −8.1 to −1.8) and −6.5 ± 0.7 (09FW37: range −8.3 to −4.9), respectively. The Hf isotopic compositions suggest that magma generation involved a significant contribution from the remelting of old continental crust material with a crustal model age of late Paleoproterozoic (T^{C}_{DM}: 1665–1784 Ma).

Whole-Rock Geochemistry. Samples from the Jiacha pluton have high SiO_2 contents of 69–71 wt% and low Al_2O_3 contents of 13.7–14.4 wt%, with A/CNK values, i.e., molar $Al_2O_3/(Na_2O + K_2O + CaO)$, of 1.00–1.08 and negative Eu anomalies (δEu: 0.55–0.61). The Langxian granodiorites possess a slightly higher SiO_2 (72–76 wt%) and lower Al_2O_3 (12.1–13.8 wt%), coupled with prominent Eu anomalies of 0.31–0.48 and A/CNK values of 1.05–1.11 (table A4; fig. 4). Three relatively more primitive samples, 09FW36, 09FW39, and 09FW54, have high Na_2O contents (3.1–4.4 wt%) and Na_2O/K_2O ratios (1.50–1.90), typical of calc-alkaline composition. These lines of evidence suggest that the Langxian granodiorites and Jiacha monzogranites belong to the I-type granites (Chappell and White 1974). The felsic dike (09FW37) has the highest SiO_2 content and lowest concentration of rare earth

Table 1. Summary of Zircon U-Pb and Hf Isotope Data of Langxian and Jiacha Plutons

Sample number	Latitude (°N)	Longitude (°E)	Lithology	Age (Ma)	Dating method	$\varepsilon_{Hf}(t)$	T^{C}_{DM} (Ma)
Jiacha pluton:							
JC01-1	29.15	92.66	Monzogranite	345.3 ± 2.6	LA-ICPMS	−5.4 ± 0.4	1691 ± 24
09FW55	29.15	92.66	Monzogranite	346.7 ± 2.7	SIMS	−4.9 ± 0.5	1665 ± 30
Langxian pluton:							
09FW36	29.07	93.08	Granodiorite	355.1 ± 4.2	LA-ICPMS	−6.8 ± 0.4	1784 ± 23
ML12-1	29.07	93.08	Granodiorite	352.0 ± 3.1	LA-ICPMS	−6.5 ± 0.7	1765 ± 46
ML12-1	29.07	93.08	Granodiorite	353.5 ± 2.6	SIMS	ND	ND
09FW35	29.07	93.08	Dioritic enclave	353.3 ± 3.2	LA-ICPMS	−5.8 ± 0.7	1725 ± 46
09FW35	29.07	93.08	Dioritic enclave	355.5 ± 2.8	SIMS	ND	ND
09FW37	29.07	93.08	Felsic dike	352.1 ± 6.9	LA-ICPMS	−6.5 ± 0.7	1769 ± 43
09FW37	29.07	93.08	Felsic dike	354.1 ± 2.9	SIMS	ND	ND

Note. The detailed data are listed in tables A1–A3, in the online edition or from the *Journal of Geology* office. LA-ICPMS = laser ablation–inductively coupled plasma mass spectrometry; ND = not determined; SIMS = secondary-ion mass spectrometry.

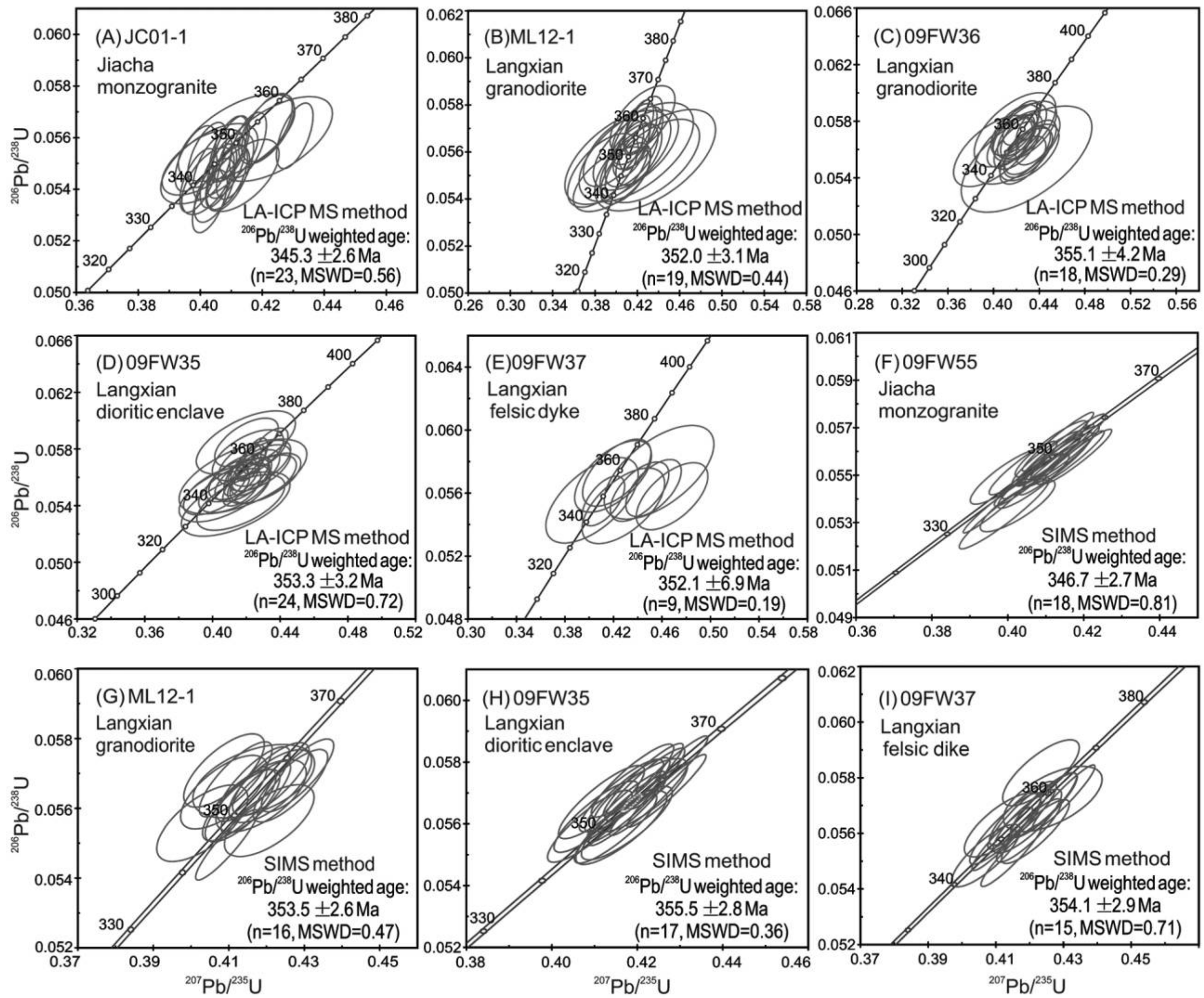

Figure 3. Zircon U-Pb concordia diagrams of Jiacha and Langxian granitoids. SIMS = secondary-ion mass spectrometry. A color version of this figure is available in the online edition or from the *Journal of Geology* office.

elements (REEs; fig. 4*A*); thus, it maybe the evolved product of coeval granitoids.

Discussion

Early Carboniferous Granitoids and Coeval Magmatism in the Lhasa Terrane. Our results suggest that the Jiacha and Langxian plutons were emplaced at 347–345 and 355–352 Ma, respectively, in the Early Carboniferous. Together with the recently reported Late Devonian deformed granite near Jiacha (~367 Ma; Dong et al. 2010*a*), the southern Lhasa terrane may be characterized by Late Devonian–Early Carboniferous granitic magmatism. In addition, Devonian-Carboniferous inherited zircons have been observed in the Gangdese batholith and associated volcanic rocks (Quidelleur et al. 1997; Lee et al. 2007; Wen et al. 2008; Chung et al. 2009; Zhu et al. 2011*b*). Moreover, Zhang et al. (2009) reported abundant Devonian-Permian (390–280 Ma) detrital zircons in river sediment sampled from a tributary of the Yarlung-Tsangbo (sample 7 of Zhang et al. 2009), north of Langxian. The tributary is short, and more than half of its zircon populations are 370–330 Ma in age, suggesting the exposure of Late Devonian–Early Carboniferous granitoids in its catchment. Most recently, Dong et al. (2010*b*) found that in the Linzhi-Milin area, many detrital zircons from the Nyingtri Group yielded late Paleozoic ages (405–290 Ma), clustering at 365–325 Ma. Although Dong et al. (2010*b*) argued that these ages may be meaningless, these zircons' good concordance and moderate Th/U ratios (most ranging from 0.4 to 1.0) indicate that they possess potential

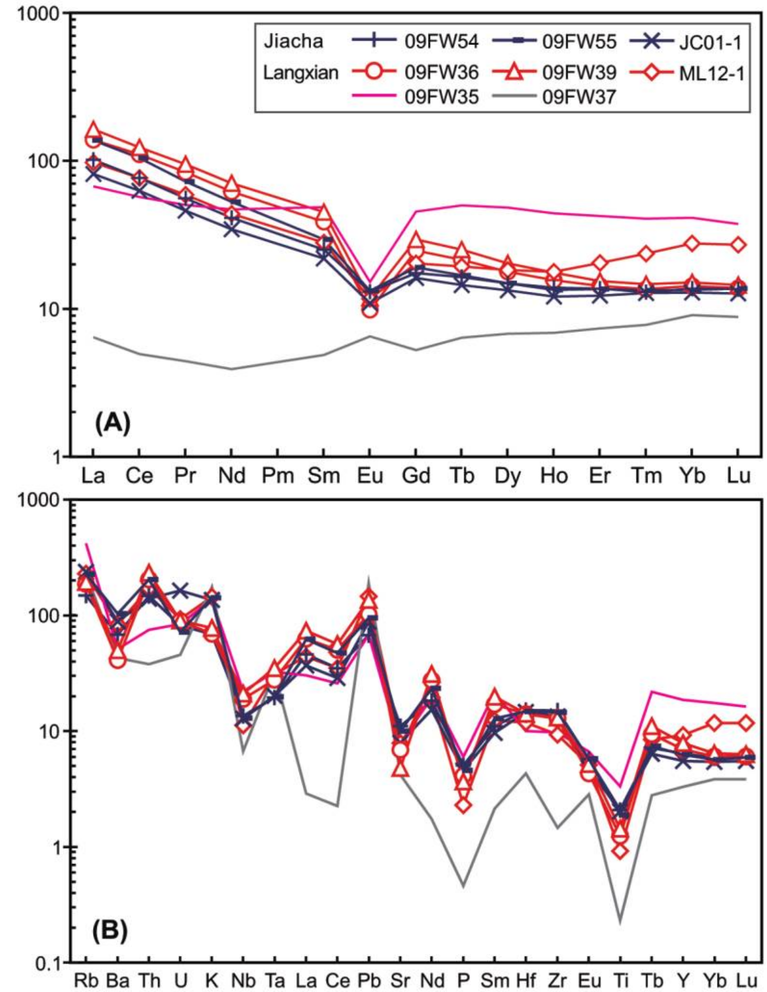

Figure 4. *A*, Chondrite-normalized rare earth element patterns. *B*, Primitive mantle–normalized trace-element spider diagrams.

geological implications, as testified by the newly identified late Paleozoic granitic rocks (Dong et al. 2010*a*; this study). The high Th/U ratios (0.2–0.7), as well as the well-developed oscillatory zoning for available zircon samples, suggest that most of these inherited and detrital zircons are of magmatic origin. In addition, all these zircons delineate a rather uniform Hf isotopic composition, with $\varepsilon_{Hf}(t)$ values from -11 to 0 (Lee et al. 2007; Chung et al. 2009; Zhang et al. 2009; Ji 2010), corresponding to those of the Jiacha and Langxian granitoids (fig. 5*A*). We therefore argue that Late Devonian–Early Carboniferous magmatism was active and perhaps more widely developed in the southern Lhasa terrane. In fact, inherited zircons with similar U-Pb ages and $\varepsilon_{Hf}(t)$ values have also been reported in Permian-Cenozoic granitic rocks from the central Lhasa terrane (fig. 5*A*; Chu et al. 2006; Zhu et al. 2009*b*, 2011*b*; Ji 2010). This implies some similarities or even a genetic link in the Late Devonian–Carboniferous magmatism and crustal evolution between the central and southern parts of the Lhasa terrane.

Late Paleozoic Geological Records and Some New Interpretations. The comparability between the central and southern parts of the Lhasa terrane is not limited to sporadic coeval magmatic records. The Hf isotope characteristics of the late Paleozoic zircons from the southern Lhasa terrane suggest that some Paleo- to Mesoproterozoic materials, by implication ancient basement, survived locally, in contrast to the universal juvenile materials there represented by the Mesozoic Gangdese batholith (fig. 5*A*, 5*B*; Guan et al. 2010, 2011; Ji 2010; Chu et al. 2011; Yang et al. 2011; Zhu et al. 2011*b*). The basement revealed by late Paleozoic inherited zircons from the central Lhasa terrane is also of Paleo-

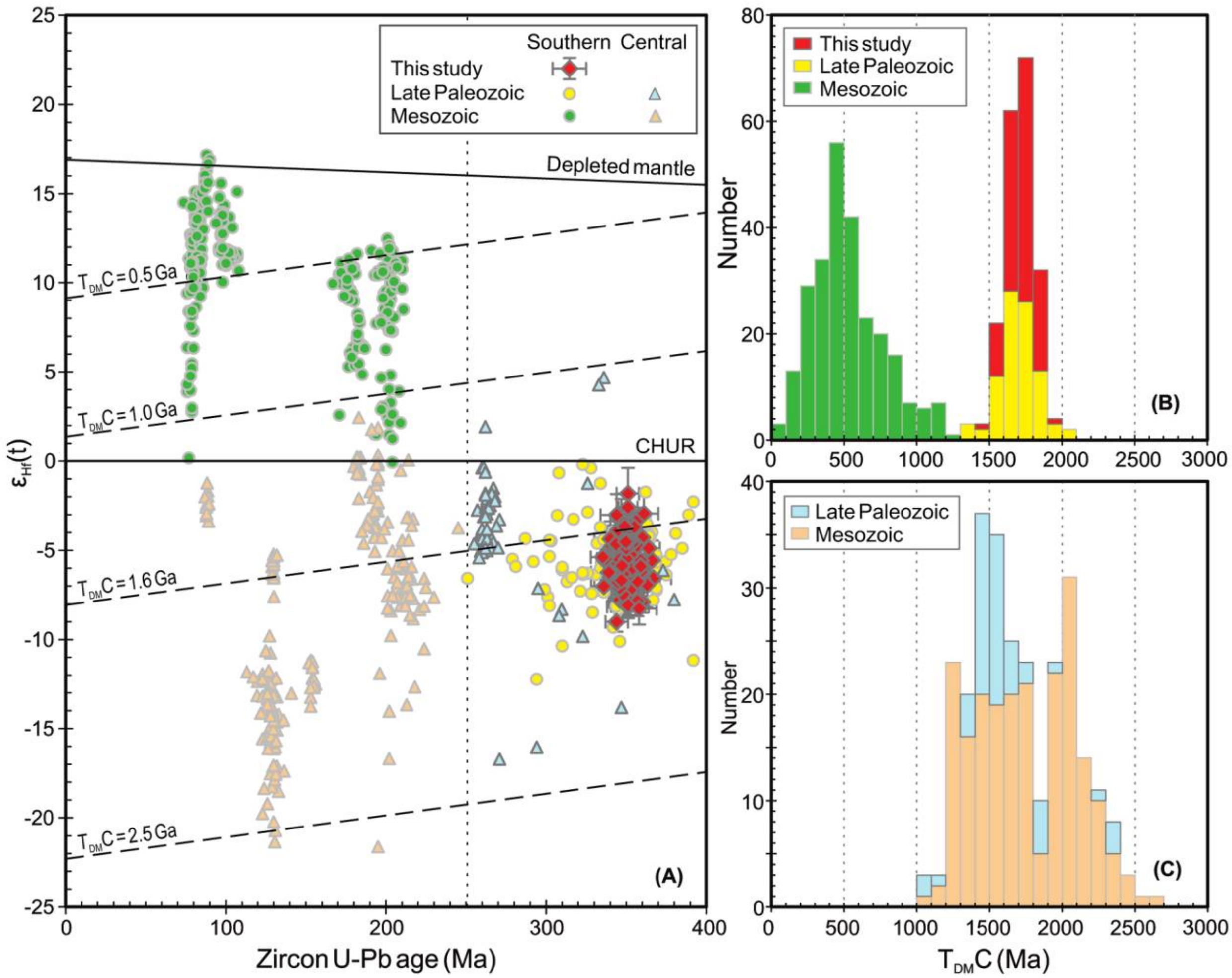

Figure 5. *A*, U-Pb age versus $\varepsilon_{Hf}(t)$ value for late Paleozoic–Mesozoic zircons from Lhasa-Linzhi region. *B*, Crustal model age (T^{C}_{DM}) of late Paleozoic and Mesozoic zircons from the southern Lhasa terrane. *C*, Crustal model age of late Paleozoic and Mesozoic zircons from the central Lhasa terrane. Data sources include (1) Early Carboniferous granitoids (this study), (2) inherited and detrital late Paleozoic zircons from the southern Lhasa terrane (Lee et al. 2007; Chung et al. 2009; Zhang et al. 2009; Ji 2010; Zhu et al. 2011*b*), (3) the Mesozoic Gangdese batholith (Guan et al. 2010, 2011; Ji 2010; Chu et al. 2011; Yang et al. 2011; Zhu et al. 2011*b*), (4) late Paleozoic zircons from the central Lhasa terrane (Chu et al. 2006; Zhu et al. 2009*b*, 2011*b*; Ji 2010), and (5) Mesozoic granitoids from the central Lhasa terrane (Meng et al. 2010; Gao et al. 2011; Zhu et al. 2011*b*). CHUR = chondrite uniform reservoir.

to Mesoproterozoic age (Chu et al. 2006; Zhu et al. 2009*b*, 2011*b*; Ji 2010), which is consistent with the studies of Permian and Mesozoic magmatic rocks there (Zhu et al. 2009*b*, 2011*b*; Meng et al. 2010; Gao et al. 2011; fig. 5*C*). Furthermore, recent studies of metasedimentary rocks from the southern (Nyingtri Group; Dong et al. 2010*b*) and central parts of the Lhasa terrane (Carboniferous-Permian metasedimentary strata; Leier et al. 2007; Zhu et al. 2011*a*) indicate that they exhibit identical detrital-zircon age frequencies (see fig. 3 in Zhu et al. 2011*c*). These lines of evidence, including coeval magmatic records and similar basement natures reflected by the Hf isotopes and detrital-zircon age frequency, suggest that the southern and central parts of the Lhasa terrane show close affinity despite the presence of a suture zone, as delineated by the Sumdo eclogite belt between them (Yang et al. 2009). Therefore, we tentatively propose that the southern and central parts of the Lhasa terrane probably had been an integrated block before the late Paleozoic.

When did the oceanic crust represented by the Sumdo eclogite come into existence, and when did subduction initiate? There is an east-west-trending Carboniferous-Permian volcanic belt in the central Lhasa terrane north of the Sumdo eclogite belt (Pan et al. 2004). A study of its genetic setting would be helpful for constraining the late Paleozoic evolution of the Lhasa terrane. Previous studies proposed a Carboniferous marginal-rifting setting (Geng et al. 2007) or a Permian arc setting (Geng et al. 2009; Yang et al. 2009; Zhu et al. 2010). The evidence that Permian volcanic rocks from the central Lhasa terrane are of the arc type is based mainly on their geochemical characteristics, such as high Al_2O_3 contents and negative Nb-Ta-Ti anomalies (Geng et al. 2009; Zhu et al. 2010).

However, we find that the volcanic rocks in the central Lhasa terrane show various geochemical compositions. The samples that possess obviously high Al_2O_3 contents are from the Middle Permian Leiqingla volcanic rocks, whereas there is no distinct difference in Al_2O_3 content between Early Permian basalts from the Tethyan Himalaya and those from the central Lhasa terrane (see fig. 3*C* in Zhu et al. 2010). Furthermore, the rock assemblages in the central Lhasa terrane differ between Early Permian, mainly basalts, and Middle Permian, from basaltic andesite to rhyolite (Geng et al. 2009; Zhu et al. 2010). In addition, some Early Permian basalts in the central Lhasa terrane exhibit a MORB-like nature (Geng et al. 2009), which is uncommon in an arc-type system. Thus, the petrogenesis of Early and Middle Permian volcanic rocks from the central Lhasa terrane may be different.

An alternative explanation for the coexistence of arc- and MORB-type rocks is that they formed in a back-arc setting. On the basis of a comprehensive study of many back-arc basalt systematics, Taylor and Martinez (2003) found a general trend from arc-like to MORB-like characteristics with increasing distance away from the subduction front. The arc-like characteristics are related to an increasing contribution from slab-derived components, including water, in the mantle wedge toward the oceanic trench, whereas the MORB-like affinity is derived from partial melting of the upwelling asthenosphere mantle. In addition, some variations also exist because of the diverse mixture of lithosphere and asthenosphere mantle sources during partial melting at different places. Water is a key factor, controlling early evolution of basaltic magma by suppressing plagioclase crystallization relative to that of olivine and clinopyroxene, which results in high Al_2O_3 content in the remnant melts. That is why high-alumina basalts (HABs) prevail in the arc volcanic system. However, some studies have found that small amounts of water in MORB and back-arc basin basalt magmas also could result in high-alumina characters (see Danyushevsky 2001). As HAB can be generated by various processes and in different settings (see Crawford et al. 1987 for a review), the existence of HAB alone is insufficient to constrain the tectonic setting.

Although it has been argued that the Early Permian basalts were formed in arc setting (Geng et al. 2009; Zhu et al. 2010), we observed that some of them display a MORB-like affinity. For example, four samples (TJ5-4–TJ5-7) of Tangjia basalt from the lower part of the Luobadui Formation (Geng et al. 2009) show low Al_2O_3 contents (14.89–15.97 wt%), flat REE patterns ($(La/Yb)_N$ = 0.81–1.10), and depleted Nd isotopic compositions ($\varepsilon_{Nd}(t)$ = 7.4–7.8; recalculated with the same parameters), similar to the values of the MORB-type Sumdo eclogite, whose Al_2O_3 contents, $(La/Yb)_N$, and $\varepsilon_{Nd}(t)$ values are 12.93–16.87 wt%, 0.21–1.42, and 7.3–8.2, respectively (Li et al. 2009*b*). In addition, we found that the basalts with more arc-like characteristics also show lower $\varepsilon_{Nd}(t)$ values. Previous studies indicated that the basement underlying the central Lhasa terrane is ancient (Zhu et al. 2011*b* and references therein); thus, its lithosphere mantle could also have enriched isotopic composition. Because this mantle source had been fertilized by slab-derived components, more involvement of such source materials during partial melting would generate basalts with an obvious arc-like nature and low $\varepsilon_{Nd}(t)$ values. The coeval developments of Early Permian MORB-like and arc-like basalts in the central Lhasa terrane, then, point to a probable back-arc setting.

In contrast to the Early Permian volcanic rocks, mainly of basaltic compositions, the Middle Permian volcanic rocks comprise various types from basaltic andesite to rhyolite and globally display obvious arc-like geochemical characteristics (Geng et al. 2009; Zhu et al. 2010), which could have resulted from later subduction of oceanic crust possibly formed during earlier back-arc spreading. Subsequently, the central Lhasa terrane collided with the southern Lhasa terrane, resulting in the Pikang granite and the regional unconformity between the middle and upper Permian in the central Lhasa terrane (Zhu et al. 2009*b*). This orogenic event ended the short-lived oceanic subduction, and then some of the deeply subducted oceanic crust was exhumed to form the Sumdo eclogite (Yang et al. 2009).

Broader Implications. Similar basement natures revealed by zircon Hf model ages (fig. 5) and the detrital-zircon age spectrum (Zhu et al. 2011*c*), together with the tectonic evolution history reflected by the characteristic of volcanic rocks, imply that the southern and central Lhasa terranes formed an integrated block before the late Paleozoic. This block underwent Carboniferous extension, Early

Permian back-arc basin spreading, subsequent short-term subduction, and block amalgamation. The Early Carboniferous granitoids from Langxian and Jiacha were derived from reworking of ancient basement in an extensional setting associated with outboard subduction. The obvious contrast in Hf isotopic composition between the late Paleozoic and early Mesozoic zircons from the southern Lhasa terrane suggests that addition of juvenile materials to the continental lithosphere was important. These juvenile source materials likely contributed much to the generation of the Gangdese batholith, as shown by their zircon Hf isotopes, whose evolutionary trend intersects the depleted mantle at the late Paleozoic–early Mesozoic era (see fig. 10 in Ji et al. 2009*a*). A possible mechanism for the crustal growth is the upwelling and partial melting of asthenosphere during a strong extension in the late Paleozoic, following a model found in similar back-arc settings (e.g., Collins 2002; Kemp et al. 2009). Some Tangjia basalts of the Early Permian exhibit obviously high Nd composition (Geng et al. 2009), confirming the input of asthenosphere materials into the crust of the Lhasa terrane. Furthermore, our results show that the Tethyan Ocean had various evolution histories along different segments of the northern margin of Gondwanaland. For example, two branches of Tethys developed where the Lhasa terrane departed (see northern Australia, as implied by characteristics of detrital zircon; Zhu et al. 2011*a*). While the northern branch separated the southern and central parts of the Lhasa terrane, as revealed by the Sumdo eclogite belt, the southern one split the amalgamated block including the southern and central Lhasa terranes away from northern Gondwanaland and subsequently changed into the Neo-Tethyan Ocean, represented by the Indus-Tsangbo suture.

ACKNOWLEDGMENTS

We are grateful to A. M. C. Şengör and D. C. Zhu for their very critical but constructive reviews and to the editor, David Rowley, for his insightful comments. We thank the staffs of the MC-ICP-MS, CAMECA IMS-1280, and x-ray fluorescence labs at the Institute of Geology and Geophysics, Chinese Academy of Sciences, for help with zircon and major-element analyses, and that of the LA-ICPMS lab at State Key Laboratory of Geological Processed and Mineral Resources, China University of Geosciences, Wuhan, for help with trace-element analyses. This study was financially supported by funds from National Natural Science Foundation of China (grants 41102035 and 41130313) and the Chinese Academy of Sciences (KZCX2-YW-Q09-06).

REFERENCES CITED

Chappell, B. W., and White, A. J. R. 1974. Two contrasting granite types. Pac. Geol. 8:173–174.

Chu, M. F.; Chung, S. L.; O'Reilly, S. Y.; Pearson, N. J.; Wu, F. Y.; Li, X. H.; Liu, D. Y.; Ji, J. Q.; Chu, C. H.; and Lee, H. Y. 2011. India's hidden inputs to Tibetan orogeny revealed by Hf isotopes of Transhimalayan zircons and host rocks. Earth Planet. Sci. Lett. 307: 479–486.

Chu, M. F.; Chung, S. L.; Song, B.; Liu, D.; O'Reilly, S. Y.; Pearson, N. J.; Ji, J. Q.; and Wen, D. J. 2006. Zircon U-Pb and Hf isotope constraints on the Mesozoic tectonics and crustal evolution of southern Tibet. Geology 34:745–748.

Chung, S. L.; Chu, M. F.; Ji, J. Q.; O'Reilly, S. Y.; Pearson, N. J.; Liu, D. Y.; Lee, T. Y.; and Lo, C. H. 2009. The nature and timing of crustal thickening in southern Tibet: geochemical and zircon Hf isotopic constraints from postcollisional adakites. Tectonophysics 477:36–42.

Chung, S. L.; Liu, D. Y.; Ji, J. Q.; Chu, M. F.; Lee, H. Y.; Wen, D. J.; Lo, C. H.; Lee, T. Y.; Qian, Q.; and Zhang, Q. 2003. Adakites from continental collision zones: melting of thickened lower crust beneath southern Tibet. Geology 31:1021–1024.

Collins, W. J. 2002. Hot orogens, tectonic switching, and creation of continental crust. Geology 30:535–538.

Coulon, C.; Maluski, H.; Bollinger, C.; and Wang, S. 1986. Mesozoic and Cenozoic volcanic rocks from central and southern Tibet: $^{39}Ar/^{40}Ar$ dating, petrological characteristics and geodynamical significance. Earth Planet. Sci. Lett. 79:281–302.

Crawford, A. J.; Falloon, T. J.; and Eggins, S. 1987. The origin of island arc high-alumina basalts. Contrib. Mineral. Petrol. 97:417–430.

Danyushevsky, L. V. 2001. The effect of small amounts of H_2O on crystallisation of mid-ocean ridge and back-arc basin magmas. J. Volcanol. Geotherm. Res. 110: 265–280.

Dong, X.; Zhang, Z. M.; Geng, G. S.; Liu, F.; Wang, W.; and Yu, F. 2010*a*. Devonian magmatism from the southern Lhasa terrane, Tibetan Plateau. Acta Petrol. Sin. 26:2226–2232 (in Chinese with English abstract).

Dong, X.; Zhang, Z. M.; and Santosh, M. 2010*b*. Zircon U-Pb chronology of the Nyingtri group, southern Lhasa terrane, Tibetan Plateau: implications for Grenvillian and Pan-African provenance and Mesozoic-Cenozoic metamorphism. J. Geol. 118:677–690.

Dong, X.; Zhang, Z. M.; Santosh, M.; Wang, W.; Yu, F.; and Liu, F. 2011. Late Neoproterozoic thermal events in the northern Lhasa terrane, South Tibet: zircon chronology and tectonic implications. J. Geodynam. 52:389–405.

Gao, Y. L.; Chen, Y. C.; Wang, C. H.; and Hou, K. J. 2011. Zircon Hf isotopic characteristics and constraints on petrogenesis of Mesozoic-Cenozoic magmatic rocks in the Nyainqentangla region, Tibet. Miner. Depos. 30: 279–291 (in Chinese with English abstract).

Geng, Q. R.; Sun, Z. M.; Pan, G. T.; Zhu, D. C.; and Wang, L. Q. 2009. Origin of the Gangdise (Transhimalaya) Permian arc in southern Tibet: stratigraphic and volcanic geochemical constraints. Isl. Arc 18:467–487.

Geng, Q. R.; Wang, L. Q.; Pan, G. T.; Jin, Z. M.; Zhu, D. C.; Liao, Z. L.; Li, G. M.; and Li, F. Q. 2007. Volcanic rock geochemistry and tectonic implication of the Luobadui formation on the Gangdese zone, Xizang (Tibet). Acta Petrol. Sin. 23:2699–2714 (in Chinese with English abstract).

Guan, Q.; Zhu, D. C.; Zhao, Z. D.; Dong, G. C.; Mo, X. X.; Liu, Y. S.; Hu, Z. C.; and Yuan, H. L. 2010. Zircon U-Pb chronology geochemistry of the Late Cretaceous mafic magmatism in the southern Lhasa terrane and its implications. Acta Petrol. Sin. 27:2083–2094 (in Chinese with English abstract).

Guan, Q.; Zhu, D. C.; Zhao, Z. D.; Zhang, L. L.; Liu, M.; Li, X. M.; Yu, F.; and Mo, X. X. 2011. Late Cretaceous adakites in the eastern segment of the Gangdese Belt, southern Tibet: products of Neo-Tethyan ridge subduction? Acta Petrol. Sin. 26:2165–2179 (in Chinese with English abstract).

He, S. D.; Kapp, P.; DeCelles, P. G.; Gehrels, G. E.; and Heizler, M. 2007. Cretaceous-Tertiary geology of the Gangdese Arc in the Linzhou area, southern Tibet. Tectonophysics 433:15–37.

Hu, D. G.; Wu, Z. H.; Jiang, W.; Shi, Y. R.; Ye, P. S.; and Liu, Q. S. 2005. SHRIMP zircon U-Pb age and Nd isotopic study on the Nyainqêntanglha group in Tibet. Sci. China Ser. D 48:1377–1386.

Ji, W. Q. 2010. Geochronology and petrogenesis of granitic rocks from east segment of the Gangdese batholith, southern Tibet. PhD thesis. Institute of Geology and Geophysics, Chinese Academy of Sciences, Beijing (in Chinese with English abstract).

Ji, W. Q.; Wu, F. Y.; Chung, S. L.; Li, J. X.; and Liu, C. Z. 2009*a*. Zircon U-Pb geochronology and Hf isotopic constraints on petrogenesis of the Gangdese batholith, southern Tibet. Chem. Geol. 262:229–245.

Ji, W. Q.; Wu, F. Y.; Liu, C. Z.; and Chung, S. L. 2009*b*. Geochronology and petrogenesis of granitic rocks in Gangdese batholith, southern Tibet. Sci. China Ser. D 52:1240–1261.

Kang, Z. Q.; Xu, J. F.; Dong, Y. H.; and Wang, B. D. 2008. Cretaceous volcanic rocks of the Zenong Group in north-middle Lhasa Block: products of southward subduction of the Slainajap Ocean? Acta Petrol. Sin. 24: 303–314 (in Chinese with English abstract).

Kemp, A. I. S.; Hawkesworth, C. J.; Collins, W. J.; Gray, C. M.; Blevin, P. L.; and EIMF (Edinburgh Ion Microprobe Facility). 2009. Isotopic evidence for rapid continental growth in an extensional accretionary orogen: the Tasmanides, eastern Australia. Earth Planet. Sci. Lett. 284:455–466.

Lee, H. Y.; Chung, S. L.; Lo, C. H.; Ji, J. Q.; Lee, T. Y.; Qian, Q.; and Zhang, Q. 2009. Eocene Neotethyan slab breakoff in southern Tibet inferred from the Linzizong volcanic record. Tectonophysics 477:20–35.

Lee, H. Y.; Chung, S. L.; Wang, Y. B.; Zhu, D. C.; Yang, J. H.; Song, B.; Liu, D. Y.; and Wu, F. Y. 2007. Age, petrogenesis and geological significance of the Linzizong volcanic successions in the Linzhou basin, southern Tibet: evidence from zircon U-Pb dates and Hf isotopes. Acta Petrol. Sin. 23:493–500.

Leier, A. L.; Kapp, P.; Gehrels, G. E.; and DeCelles, P. G. 2007. Detrital zircon geochronology of Carboniferous-Cretaceous strata in the Lhasa terrane, southern Tibet. Basin Res. 19:361–378.

Li, X. H.; Li, W. X.; Wang, X. C.; Li, Q. L.; Liu, Y.; and Tang, G. Q. 2009*a*. Role of mantle-derived magma in genesis of early Yanshanian granites in the Nanling Range, south China: in situ zircon Hf-O isotopic constraints. Sci. China Ser. D 52:1262–1278.

Li, Z. L.; Yang, J. S.; Xu, Z. Q.; Li, T. F.; Xu, X. Z.; Ren, Y. F.; and Robinson, P. T. 2009*b*. Geochemistry and Sm-Nd and Rb-Sr isotopic composition of eclogite in the Lhasa terrane, Tibet, and its geological significance. Lithos 109:240–247.

Liu, Y. S.; Hu, Z. C.; Gao, S.; Günther, D.; Xu, J.; Gao, C. G.; and Chen, H. H. 2008. In situ analysis of major and trace elements of anhydrous minerals by LA-ICP-MS without applying an internal standard. Chem. Geol. 257:34–43.

Meng, F. Y.; Zhao, Z. D.; Zhu, D. C.; Zhang, L. L.; Guan, Q.; Liu, M.; Yu, F.; and Mo, X. X. 2010. Petrogenesis of Late Cretaceous adakite-like rocks in Mamba from the eastern Gangdese, Tibet. Acta Petrol. Sin. 26: 2180–2192 (in Chinese with English abstract).

Mo, X. X.; Dong, G. C.; Zhao, Z. D.; Zhou, S.; Wang, L. L.; Qiu, R. Z.; and Zhang, F. Q. 2005. Spatial and temporal distribution and characteristics of granitoids in the Gangdese, Tibet and implication for crustal growth and evolution. Geol. J. China Univ. 11:281–290 (in Chinese with English abstract).

Pan, G. T.; Ding, J.; Yao, D. S.; and Wang, L. Q. 2004. Guidebook of the 1 : 1,500,000 geologic map of the Qinghai-Xizang (Tibet) Plateau and adjacent areas. Chengdu Cartographic, Chengdu, 148 p.

Quidelleur, X.; Grove, M.; Lovera, O. M.; Harrison, T.; Yin, A.; and Ryerson, F. J. 1997. Thermal evolution and slip history of the Renbu Zedong thrust, southeastern Tibet. J. Geophys. Res. 102:2659–2679.

Schärer, U.; Xu, R. H.; and Allègre, C. J. 1984. U-Pb geochronology of Gandese (Transhimalaya) plutonism in the Lhasa-Xigaze region, Tibet. Earth Planet. Sci. Lett. 69:311–320.

Şengör, A. M. C.; Altıner, D.; Cin, A.; Ustaömer, T.; and Hsü, K. J. 1988. Origin and assembly of the Tethyside orogenic collage at the expense of Gondwana-land. *In* Audley-Charles, M. G., and Hallam, A., eds. Gondwana and Tethys. Geol. Soc. Lond. Spec. Publ. 37:119–181.

Taylor, B., and Martinez, F. 2003. Back-arc basin basalt systematics. Earth Planet. Sci. Lett. 210:481–497.

Wen, D. R.; Chung, S. L.; Song, B.; Iizuka, Y.; Yang, H.

J.; Ji, J. Q.; Liu, D. Y.; and Gallet, S. 2008. Late Cretaceous Gangdese intrusions of adakitic geochemical characteristics, SE Tibet: petrogenesis and tectonic implications. Lithos 105:1–11.

Wu, F. Y.; Yang, Y. H.; Xie, L. W.; Yang, J. H.; and Xu, P. 2006. Hf isotopic compositions of the standard zircons and baddeleyites used in U-Pb geochronology. Chem. Geol. 234:105–126.

Xie, L. W.; Zhang, Y. B.; Zhang, H. H.; Sun, J. F.; and Wu, F. Y. 2008. *In situ* simultaneous determination of trace elements, U-Pb and Lu-Hf isotopes in zircon and baddeleyite. Chin. Sci. Bull. 53:1565–1573.

Yang, J. S.; Xu, Z. Q.; Li, Z. L.; Xu, X. Z.; Li, T. F.; Ren, Y. F.; Li, H. Q.; Chen, S. Y.; and Robinson, P. T. 2009. Discovery of an eclogite belt in the Lhasa block, Tibet: a new border for Paleo-Tethys? J. Asian Earth Sci. 34: 76–89.

Yang, Z. M.; Hou, Z. Q.; Jiang, Y. F.; Zhang, H. R.; and Song, Y. C. 2011. Sr-Nd-Pb and zircon Hf isotopic constraints on petrogenesis of the Late Jurassic granitic porphyry at Qulong, Tibet. Acta Petrol. Sin. 27:2003–2010.

Yin, A., and Harrison, T. M. 2000. Geologic evolution of the Himalayan-Tibetan orogen. Annu. Rev. Earth Planet. Sci. 28:211–280.

Zhang, J. Y.; Yin, A.; Wu, F. Y.; Dai, J. G.; and Liu, W. 2009. Coupled U-Pb dating and Hf isotopic analysis of detrital zircons from modern sand of the Yalu River system (Yarlung Tsangpo) in southern Tibet: implications for Himalayan provenance analysis and drainage reconstruction. American Geophysical Union, Fall Meeting 2009, abstract #T43B-2072.

Zhang, Z. M.; Dong, X.; Geng, G. S.; Wang, W.; Yu, F.; and Liu, F. 2010. Precambrian metamorphism of the northern Lhasa terrane, south Tibet and its tectonic implications. Acta Geol. Sin. 84:449–456 (in Chinese with English abstract).

Zhu, D. C.; Mo, X. X.; Niu, Y. L.; Zhao, Z. D.; Wang, L. Q.; Liu, Y. S.; and Wu, F. Y. 2009*a*. Geochemical investigation of early Cretaceous igneous rocks along an east-west traverse throughout the central Lhasa terrane, Tibet. Chem. Geol. 268:298–312.

Zhu, D. C.; Mo, X. X.; Niu, Y. L.; Zhao, Z. D.; Yang, Y. H.; and Wang, L. Q. 2009*b*. Zircon U-Pb dating and *in-situ* Hf isotopic analysis of Permian peraluminous granite in the Lhasa terrane, southern Tibet: implications for Permian collisional orogeny and paleogeography. Tectonophysics 469:48–60.

Zhu, D. C.; Mo, X. X.; Zhao, Z. D.; Niu, Y. L.; Wang, L. Q.; Chu, Q. H.; Pan, G. T.; Xu, J. F.; and Zhou C. Y. 2010. Presence of Permian extension- and arc-type magmatism in southern Tibet: paleogeographic implications. Geol. Soc. Am. Bull. 122:979–993.

Zhu, D. C.; Pan, G. T.; Chung, S. L.; Liao, Z. L.; Wang, L. Q.; and Li, G. M. 2008. SHRIMP zircon age and geochemical constraints on the origin of Early Jurassic volcanic rocks from the Yeba formation, southern Gangdese in south Tibet. Int. Geol. Rev. 50:442–471.

Zhu, D. C.; Pan, G. T.; Zhao, Z. D.; Lee, H. Y.; Kang, Z. Q.; Liao, Z. L.; Wang, L. Q.; Li, G. M.; Dong, G. C.; and Liu, B. 2009*c*. Early Cretaceous subduction-related adakite-like rocks in the Gangdese, south Tibet: products of slab melting and subsequent melt-peridotite interaction? J. Asian Earth Sci. 34:298–309.

Zhu, D. C.; Zhao, Z. D.; Niu, Y. L.; Dilek, Y.; and Mo, X. X. 2011*a*. Lhasa terrane in southern Tibet came from Australia. Geology 39:727–730.

Zhu, D. C.; Zhao, Z. D.; Niu, Y. L.; Mo, X. X.; Chung, S. L.; Hou, Z. Q.; Wang, L. Q.; and Wu, F. Y. 2011*b*. The Lhasa terrane: record of a microcontinent and its histories of drift and growth. Earth Planet. Sci. Lett. 301:241–255.

Zhu, D. C.; Zhao, Z. D.; Niu, Y. L.; Wang, Q.; Dilek, Y.; Guan, Q.; Liu, Y. S.; and Mo, X. X. 2011*c*. Tracing the provenance of inherited zircons from peraluminous granites in the Lhasa terrane and its paleogeographic implications. Acta Petrol. Sin. 27:1917–1930 (in Chinese with English abstract).